



ELSEVIER

Available online at www.sciencedirect.com

SCIENCE @ DIRECT®

Journal of Sound and Vibration 286 (2005) 981–999

JOURNAL OF
SOUND AND
VIBRATION

www.elsevier.com/locate/jsvi

Love wave in ZnO/SiO₂/Si structure with initial stresses

J. Su, Z.B. Kuang*, H. Liu

Department of Engineering Mechanics, Shanghai Jiaotong University, Shanghai 200240, PR China

Received 4 August 2003; received in revised form 4 August 2004; accepted 25 October 2004

Available online 5 January 2005

Abstract

The propagation of elastic waves in the layered piezoelectric media with inhomogeneous initial stresses was analyzed through the method of transfer matrix. Firstly, the governing equations of motion for the prestressed piezoelectric media are derived on the basis of the nonlinear continuum mechanics. Secondly, the transfer matrix for the Love waves in the piezoelectric media (ZnO/SiO₂/Si structure) is presented. Solutions are obtained by the transfer matrix method. Thirdly, numerical calculations are given for the ZnO/SiO₂/Si structure. It is found that the middle layer SiO₂ and the initial stress in layers affect the phase velocity, group velocity and electromechanical coupling coefficient obviously. These results are important in the surface acoustic wave devices.

© 2004 Elsevier Ltd. All rights reserved.

1. Introduction

Investigations on the propagation of elastic waves, especially the surface acoustic wave, in layered piezoelectric media have been of great interest since films deposited on supporting substrates are generally a requisite for acoustic devices [1]. Typically, a layered structure consists of two, three or arbitrary layers of different materials. The direct method is complex for a multilayer structure. For a layered media with arbitrary layers, the transfer matrix method is a simple and powerful technique to analyze wave phenomena. The transfer matrix method was first presented by Thomson [2]. Liu et al. [3] applied this method to anisotropic laminates. Following their work, there were many works with this method. The main developments of the matrix

*Corresponding author. Tel.: +86 21 54743067; fax: +86 21 54743044.

E-mail address: zbkuang@mail.sjtu.edu.cn (Z.B. Kuang).

techniques can be attributed to Liu and Tani [4], Stewart and Yong [5], Levesque and Piche [6], Lowe [7], and Liu et al. [8].

The initial stresses in the film are inevitable and important because they may result in frequency shift, a change in the velocity of surface waves and controlling the selectivity of a filter and temperature compensation of the devices. The elastic wave propagation in a homogeneously stressed medium has been investigated by Nalamwar and Epstein [9]. Ono et al. [10] discussed the surface acoustic wave in a three layered structure without initial stress. It is, however, well known that in most practical situations the actual initial stresses have maximum values at the surface of the film and decrease rapidly along the thickness direction of the film structure. Many researchers [11,12] resorted to the perturbation theory to treat the inhomogeneous initial states. The present study involves the application of the transfer matrix method to analyze the effect of initial stress on the Love wave mode and dispersion behavior in a layered piezoelectric ceramic with thin layers deposited on a relatively thick substrate. Most Love wave sensors are fabricated on this kind of structure and have many applications, such as measuring properties of liquids [13]. The middle layer in a multi-layer structure can be used to adjust the range of phase velocity of SAW and to improve its property, such as ZnO/SiO₂/Si [14,15] structure and ZnO/Diamond/Si structure [16].

2. Equations of motion in the prestressed piezoelectric media

When a continuum medium undergoes deformation, the deformation and motion of a material point can be described by [17]

$$x_k = x_k(X_K, t), \quad K = \text{I, II, III}, \quad k = 1, 2, 3, \tag{1}$$

where the capital letter X denotes a particle position at the natural undeformed configuration and the lower letter x denotes its position at current configuration. The capital and lower subscripts K and k denote the components in the Lagrangian coordinate system at undeformed configuration and the Eulerian coordinate system at current configuration, respectively. t denotes time. Eq. (1) may be interpreted as a mapping of the natural configuration on the current configuration. The gradient equations are

$$E_K = -\Phi_{,K}, \tag{2}$$

$$\varepsilon_{KL} = \frac{1}{2}(x_{k,K}x_{k,L} - \delta_{KL}). \tag{3}$$

It is well known that the basic equations in the undeformed configuration are [17] the equations of motion:

$$(\sigma_{KL}x_{l,L})_{,K} + \rho_0 f_l = \rho_0 \ddot{u}_l, \tag{4a}$$

the electric displacement equation without volume charge

$$D_{K,K} = 0 \tag{4b}$$

and the associated boundary conditions:

$$\sigma_{KL}x_{l,L}N_K = \bar{\Sigma}_l \quad \text{on } A_T, \tag{5a}$$

$$D_K N_K = \sigma^* \quad \text{on } A_q. \tag{5b}$$

The displacement and electric potential boundary conditions are not discussed. Therefore, they are not given in this paper.

In Eqs. (2)–(5), $\boldsymbol{\sigma}$ stands for the second Piola–Kirchhoff stress tensor, $\boldsymbol{\epsilon}$ is the Green strain tensor, \mathbf{D} and \mathbf{E} are the electric displacement and electric field vectors, respectively, ρ_0 is the mass density, A_T and A_q denote the boundary surfaces subjected to external mechanical force and electrical charge, respectively. \mathbf{f} is the force per unit mass, $\bar{\Sigma}_l$ and σ^* are, respectively, the applied surface traction and surface electric charge density, Φ is the scalar electric potential. All the above variables are measured at the natural configuration. δ_{KL} is the Kronecker delta; a comma at the subscript position denotes the differentiation with respect to the space-coordinate, a dot over the letter denotes the time differentiation.

In practical cases, a mechanical biasing state produced by initial stress is in an equilibrium state. The initial stresses are produced in the manufacturing process. All the physical variables in the biasing state are designated by a superscript label “0”. According to Eq. (4), the equations of equilibrium at the initial biasing state are written as [8,17]

$$(\sigma_{KL}^0 x_{l,L}^0)_{,K} + \rho_0 f_l^0 = 0, \quad D_{K,K}^0 = 0 \tag{6}$$

and the material gradient is

$$x_{l,L}^0 = \delta_{lL} + u_{l,L}^0. \tag{7}$$

Substituting Eq. (7) into Eq. (6), it is found that

$$(\sigma_{KL}^0 \delta_{lL} + \sigma_{KL}^0 u_{l,L}^0)_{,K} + \rho_0 f_l^0 = 0. \tag{8}$$

Under the applied external dynamic mechanical and electrical loads, the body is further perturbed by an additional wave motion of small amplitude onto the biasing state. Let

$$\sigma'_{KL} = \sigma_{KL}^0 + \sigma_{KL}, \quad u'_l = u_l^0 + u_l, \quad D'_K = D_K^0 + D_K, \tag{9}$$

where σ'_{KL} and D'_K are the total Kirchhoff stress and total electric displacement referred to the natural state and u'_l is the total displacement component at Euler coordinate system. u_l , σ_{KL} and D_K are their incremental values due to the dynamic disturbance or applied signals superposed onto the biasing state. Then the equations of motion may be expressed as

$$[(\sigma_{KL}^0 + \sigma_{KL})\delta_{lL} + (\sigma_{KL}^0 + \sigma_{KL})(u_{l,L}^0 + u_{l,L})]_{,K} + \rho_0(f_l^0 + f_l) = \rho_0 \ddot{u}_l. \tag{10}$$

Subtracting Eq. (8) from Eq. (10), we obtain the expected equation of perturbed motion in the natural configuration

$$(\sigma_{KL}\delta_{lL} + \sigma_{KL}u_{l,L}^0 + u_{l,L}\sigma_{KL}^0 + \sigma_{KL}u_{l,L})_{,K} + \rho_0 f_l = \rho_0 \ddot{u}_l. \tag{11}$$

Due to the fact that σ_{KL} is small compared to σ_{KL}^0 and u_l is small compared to u_l^0 , their product term $\sigma_{KL}u_{l,L}$ is negligibly small and will be dropped. Eq. (11) is reduced to

$$(\sigma_{KL}\delta_{lL} + \sigma_{KL}u_{l,L}^0 + u_{l,L}\sigma_{KL}^0)_{,K} + \rho_0 f_l = \rho_0 \ddot{u}_l. \tag{12}$$

This is the governing wave equation of the applied signal or a perturbation in the form of a second Piola–Kirchhoff stress.

In practical calculation, the Eulerian coordinate system is adopted to coincide with the Lagrangian coordinate system for convenience. Thus Eq. (12) can be rewritten as

$$(\sigma_{ij} + \sigma_{ik}u_{j,k}^0 + u_{j,k}\sigma_{ik}^0)_{,i} + \rho_0 f_j = \rho_0 \ddot{u}_j, \quad i, j, k = 1, 2, 3. \tag{13}$$

The electric displacement equation (4b) and associated boundary conditions (5) can also be written as

$$\begin{aligned} D_{i,i} &= 0, \\ (\sigma_{ij} + \sigma_{ik}u_{j,k}^0 + u_{j,k}\sigma_{ik}^0)N_i &= \bar{\Sigma}_j \quad \text{on } A_T, \\ D_i N_i &= \sigma^* \quad \text{on } A_q, \end{aligned} \tag{14}$$

where D_i , $\bar{\Sigma}_j$ and σ^* are corresponding increments due to the dynamic disturbance superposed on the biasing state.

The constitutive equations are [17–19]

$$\begin{aligned} \sigma_{ij}^t &= c_{ijkl}\varepsilon_{kl}^t + \frac{1}{2}c_{ijklmn}\varepsilon_{kl}^t\varepsilon_{mn}^t - e_{mij}E_m^t - e_{mijkl}\varepsilon_{kl}^tE_m^t - \frac{1}{2}l_{mnij}E_m^tE_n^t + \text{h.o.t.}, \\ D_m^t &= e_{mij}\varepsilon_{ij}^t + \frac{1}{2}e_{mijkl}\varepsilon_{ij}^t\varepsilon_{kl}^t + \varepsilon_{mn}E_n^t + \frac{1}{2}\varepsilon_{mnp}E_n^tE_p^t + l_{mnij}E_n^t\varepsilon_{ij}^t + \text{h.o.t.}, \end{aligned} \tag{15}$$

where $i, j, k, l, m, n, p = 1, 2, 3$, c_{ijkl} and c_{ijklmn} are the second- and third-order elastic constants, respectively, e_{mij} and e_{mijkl} are the second- and third-order piezoelectric constants, respectively, ε_{mn} and ε_{mnp} are the second- and third-order dielectric constants, respectively, and l_{mnij} is the electrostrictive constant.

The constitutive equations for the biasing state are

$$\begin{aligned} \sigma_{ij}^0 &= c_{ijkl}\varepsilon_{kl}^0 + \frac{1}{2}c_{ijklmn}\varepsilon_{kl}^0\varepsilon_{mn}^0 - e_{mij}E_m^0 - e_{mijkl}\varepsilon_{kl}^0E_m^0 - \frac{1}{2}l_{mnij}E_m^0E_n^0 + \text{h.o.t.}, \\ D_m^0 &= e_{mij}\varepsilon_{ij}^0 + \frac{1}{2}e_{mijkl}\varepsilon_{ij}^0\varepsilon_{kl}^0 + \varepsilon_{mn}E_n^0 + \frac{1}{2}\varepsilon_{mnp}E_n^0E_p^0 + l_{mnij}E_n^0\varepsilon_{ij}^0 + \text{h.o.t.} \end{aligned} \tag{16}$$

From the difference of Eqs. (15) and (16), and on expressing the strain tensor and the electric field in terms of the displacement and electric potential gradients, respectively, one can derive a constitutive equation for the incremental stress tensor σ_{ij} and electric displacement D_m . Neglecting the higher order terms we have,

$$\begin{aligned} \sigma_{ij} &= \hat{c}_{ijkl}u_{k,l} + \hat{e}_{mij}\Phi_{,m}, \\ D_m &= e_{mij}^*u_{i,j} - \varepsilon_{mn}^*\Phi_{,n}, \end{aligned} \tag{17}$$

where

$$\begin{aligned} \hat{c}_{ijkl} &= c_{ijkl} + (c_{ijnl}\delta_{km} + c_{ijklmn})u_{m,n}^0 + e_{mijkl}\Phi_{,m}^0, & \hat{e}_{mij} &= e_{mij} + e_{mijkl}u_{k,l}^0 - l_{mnij}\Phi_{,n}^0, \\ e_{mij}^* &= e_{mij} + (e_{mil}\delta_{jk} + e_{mijkl})u_{k,l}^0 - l_{mnij}\Phi_{,n}^0, & \varepsilon_{mn}^* &= \varepsilon_{mn} + l_{mnij}u_{i,j}^0 - \varepsilon_{mnp}\Phi_{,p}^0. \end{aligned} \tag{18}$$

Substituting of Eq. (17) into Eq. (13), one obtains

$$[(\hat{c}_{ijkl} + c_{inkl}\delta_{jm}u_{m,n}^0)u_{k,l} + e_{mij}^*\Phi_{,m} + u_{j,k}\sigma_{ik}^0]_{,i} + \rho_0 f_j = \rho_0 \ddot{u}_j. \tag{19}$$

If we denote $c_{ijkl}^* = \hat{c}_{ijkl} + c_{inkl}\delta_{jm}u_{m,n}^0$, then Eqs. (13) and (14) can be rewritten as

$$(\sigma_{ij}^* + u_{j,k}\sigma_{ik}^0)_{,i} + \rho_0 f_j = \rho_0 \ddot{u}_j, \tag{20a}$$

$$D_{i,i} = 0, \tag{20b}$$

$$(\sigma_{ij}^* + u_{j,k}\sigma_{ik}^0)N_i = \bar{T}_j, \tag{20c}$$

$$D_i N_i = \sigma^*, \tag{20d}$$

where σ_{ij}^* is not the true σ_{ij} and

$$\begin{aligned} \sigma_{ij}^* &= c_{ijkl}^* u_{k,l} + e_{mij}^* \Phi_{,m} = \sigma_{ij} + c_{inkl} u_{j,l}^0 u_{k,l} + e_{mil} u_{j,l}^0 \Phi_{,m}, \\ D_m &= e_{mij}^* u_{i,j} - \epsilon_{nm}^* \Phi_{,n}, \end{aligned} \tag{21}$$

where c_{ijkl}^* , e_{mij}^* and ϵ_{nm}^* are effective elastic, piezoelectric and dielectric constants, respectively, and they are related to the initial displacement and electric potential gradients in the biasing state. If $u_{i,j}^0$ is small, then $\sigma_{ij}^* = \sigma_{ij}$. In the following text for convenience, σ_{ij}^* is replaced by σ_{ij} , but it should be noted that they are different from those σ_{ij} in previous equations.

Eqs. (20) and (21) are the fundamental governing equations and boundary conditions of applied signal or perturbation for a general prestressed piezoelectric media.

3. Transfer matrix method

In this paper we discuss that the structure is made up of two layers with thickness of h_1 and h_2 ($h_1 + h_2 = h$), respectively, which are normal to the x -axis and a substrate, as shown in Fig. 1. The symbols x, y, z are employed to represent the rectangular Cartesian coordinate system, which are

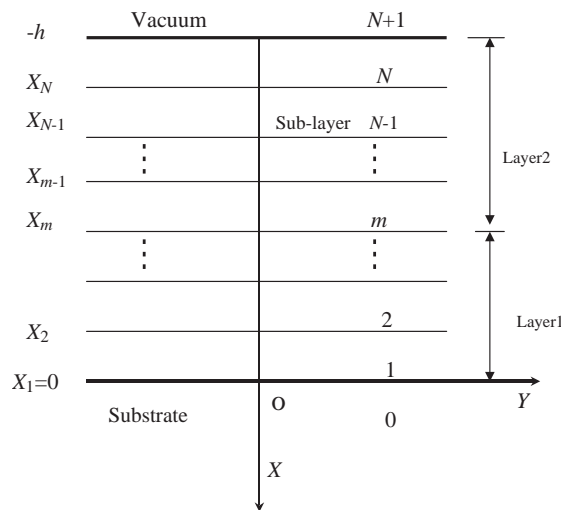


Fig. 1. The layer structure divided into N sublayers.

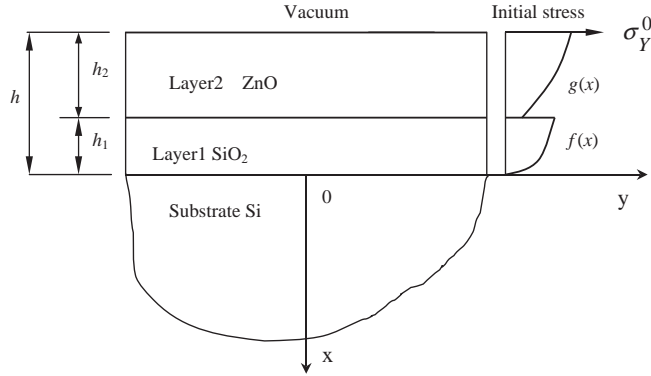


Fig. 2. Three layer structure.

equivalent to the compact form of the indicial notation x_i ($i = 1, 2, 3$). The layers are in the region $-h < x < 0$ and the substrate $x > 0$. The top surface of the layer $x = -h$ is free of stresses and charge. There exist inhomogeneously distributed initial stresses in the layers. Experiments show that the initial stresses vary along the depth x and get their peak values at the surface $x = -h$ or $-h_1$, as shown in Fig. 2. The thickness of the substrate is considerably larger than h and can be treated as a half-space. The layers can be further divided into N sublayers. 1– m sublayers belong to layer 1, $m + 1$ – N sublayers belong to layer 2. The half-space noted 0 is the substrate and the air is denoted by layer $N + 1$ (Fig. 1).

The transfer matrix method is used to solve the problem [5]. The basis for the transfer matrix method is to develop a transfer matrix for each sublayer m , which maps displacements, stress tractions, electric potential and electric charge from the lower surface of the sublayer m to its upper surface. Successive application of the transfer matrix through 0 to $N + 1$ and invoking corresponding interface continuity conditions at their interfaces lead to a set of equations relating the boundary conditions from the first interface to the last interface. After introducing the external boundary conditions at the last interface, the transfer matrix is founded.

We will utilize a state space approach, which is a kind of transfer matrix method [20]. This approach reduces the wave propagation problem to a set of first-order matrix differential equations. According to Eq. (20a), in every sublayer we have

$$\sigma_{i1,1} = \rho_0 \ddot{u}_i - \sigma_{i2,2} - \sigma_{i3,3} - u_{i,kj} \sigma_{kj}^0 - u_{i,k} \sigma_{jk,j}^0, \quad i, j, k = 1, 2, 3 \tag{22}$$

when the body force is absent.

The constitutive relation equation (21) for the piezoelectric media can be rewritten as

$$\begin{aligned} \sigma_{ij} &= c_{ijp}^* u_{p,l}, \\ D_i &= e_{ip}^* u_{p,l}, \end{aligned} \quad i, j, l = 1, 2, 3, \quad p = 1, 2, 3, 4, \tag{23}$$

where $u_4 = \Phi$, and $c_{ij4l}^* = e_{ij}^*$, $e_{i4l}^* = -\epsilon_{il}^*$. In all the following statements we define $p = 1, 2, 3, 4$, $i, j, l = 1, 2, 3$ and $\alpha, \beta, \gamma = 2, 3$.

If we identify the plane of incidence to be the plane yz as shown in Fig. 1, the solution is

$$u_p = A_p(x) \exp[i(\kappa_y y + \kappa_z z - \omega t)] = A_p(x) \exp[i(\kappa_\alpha x_\alpha - \omega t)], \tag{24}$$

where $i = \sqrt{-1}$, κ_y and κ_z are wave numbers in the y and z directions, respectively, and ω is the circular frequency.

Substitution of Eqs. (23), (24) into Eq. (22) results in

$$\begin{aligned} \sigma_{i1,1} = & [-\rho_0\omega^2 A_i - i\kappa_\beta(c_{i\beta p1}^* A_{p,1} + i\kappa_\gamma c_{i\beta p\gamma}^* A_p) - A_{i,11}\sigma_{11}^0 - i\kappa_\gamma 2A_{i,1}\sigma_{1\gamma}^0 \\ & + \kappa_\beta\kappa_\gamma\sigma_{\beta\gamma}^0 A_i - \sigma_{j1,j}^0 A_{i,1} - i\kappa_\beta\sigma_{j\beta,j}^0 A_i] \exp[i(\kappa_\alpha x_\alpha - \omega t)]. \end{aligned} \tag{25}$$

As a matter of fact, the stresses between layers σ_{11}^0 , σ_{12}^0 , σ_{13}^0 are small and can be dropped. Let

$$\sigma_{ij} = \tilde{\sigma}_{ij}(x) \exp[i(\kappa_\alpha x_\alpha - \omega t)],$$

$$D_i = T_{i+6}(x) \exp[i(\kappa_\alpha x_\alpha - \omega t)]. \tag{26}$$

Eq. (25) can be rewritten as

$$\tilde{\sigma}_{i1,1} + i\kappa_\beta c_{i\beta p1}^* A_{p,1} + \sigma_{j1,j}^0 A_{i,1} = (-\rho_0\omega^2 + \kappa_\beta\kappa_\gamma\sigma_{\beta\gamma}^0 - i\kappa_\beta\sigma_{j\beta,j}^0) A_i + \kappa_\beta\kappa_\gamma c_{i\beta p\gamma}^* A_p. \tag{27a}$$

Eqs. (20b) and (23) can be written in a similar way as

$$T_{7,1} + i\kappa_\beta e_{\beta p1}^* A_{p,1} = \kappa_\beta\kappa_\gamma e_{\beta p\gamma}^* A_p, \tag{27b}$$

$$c_{1jp1}^* A_{p,1} = \tilde{\sigma}_{j1} - i\kappa_\beta c_{1j\beta}^* A_p, \tag{27c}$$

$$e_{1p1}^* A_{p,1} = T_7 - i\kappa_\beta e_{1p\beta}^* A_p. \tag{27d}$$

In order to express Eqs. (27) as a matrix, let

$$\sigma_n = T_n(x) \exp[i(\kappa_\alpha x_\alpha - \omega t)], \quad n = 1, 2, \dots, 6,$$

where σ_n ($n = 1, 2, \dots, 6$) represents $\sigma_{11}(\sigma_x)$, $\sigma_{22}(\sigma_y)$, $\sigma_{33}(\sigma_z)$, $\sigma_{32}(\sigma_{yz})$, $\sigma_{31}(\sigma_{zx})$ and $\sigma_{12}(\sigma_{xy})$, respectively. The terms $(\tilde{\sigma}_{i1})$ in Eqs. (27a), (27c) are replaced by T_1 , T_6 and T_5 , respectively, as i changes from 1 to 3.

Eqs. (27) are the state equations and in a state space eight-dimensional unknown vectors can be defined as

$$\mathbf{v}_m(x) = (A_{1m}, A_{2m}, A_{3m}, A_{4m}, T_{1m}, T_{6m}, T_{5m}, T_{7m})^T, \tag{28}$$

where \mathbf{v} is the state vector, the subscript “ m ” indicates the quantities in the sublayer m . Then, Eq. (27) can be expressed as

$$\left(\mathbf{B}_m(x) \frac{d}{dx} - \mathbf{F}_m(x) \right) \mathbf{v}_m(x) = 0 \quad \text{or} \quad \left(\frac{d}{dx} - \mathbf{B}_m^{-1}(x) \mathbf{F}_m(x) \right) \mathbf{v}_m(x) = 0, \tag{29}$$

where $\mathbf{B}_m^{-1}(x)\mathbf{F}_m(x)$ is the state matrix of the sublayer m , where

$$\mathbf{B}_m = \begin{bmatrix} \mathbf{B}_m(1, 1) & i\kappa_\beta c_{1\beta 21}^* & i\kappa_\beta c_{1\beta 31}^* & i\kappa_\beta c_{1\beta 41}^* & 1 & 0 & 0 & 0 \\ i\kappa_\beta c_{2\beta 11}^* & \mathbf{B}_m(2, 2) & i\kappa_\beta c_{2\beta 31}^* & i\kappa_\beta c_{2\beta 41}^* & 0 & 1 & 0 & 0 \\ i\kappa_\beta c_{3\beta 11}^* & i\kappa_\beta c_{3\beta 21}^* & \mathbf{B}_m(3, 3) & i\kappa_\beta c_{3\beta 41}^* & 0 & 0 & 1 & 0 \\ i\kappa_\beta e_{\beta 11}^* & i\kappa_\beta e_{\beta 21}^* & i\kappa_\beta e_{\beta 31}^* & i\kappa_\beta e_{\beta 41}^* & 0 & 0 & 0 & 1 \\ c_{1111}^* & c_{1121}^* & c_{1131}^* & c_{1141}^* & 0 & 0 & 0 & 0 \\ c_{1211}^* & c_{1221}^* & c_{1231}^* & c_{1241}^* & 0 & 0 & 0 & 0 \\ c_{1311}^* & c_{1321}^* & c_{1331}^* & c_{1341}^* & 0 & 0 & 0 & 0 \\ e_{111}^* & e_{121}^* & e_{131}^* & e_{141}^* & 0 & 0 & 0 & 0 \end{bmatrix}, \tag{30}$$

$$\mathbf{B}_m(1, 1) = \sigma_{j1,j}^0 + i\kappa_\beta c_{1\beta 11}^*, \quad \mathbf{B}_m(2, 2) = \sigma_{j1,j}^0 + i\kappa_\beta c_{2\beta 21}^*, \quad \mathbf{B}_m(3, 3) = \sigma_{j1,j}^0 + i\kappa_\beta c_{3\beta 31}^*,$$

$$\mathbf{F}_m = \begin{bmatrix} \mathbf{F}_m(1, 1) & \kappa_\beta \kappa_\gamma c_{1\beta 2\gamma}^* & \kappa_\beta \kappa_\gamma c_{1\beta 3\gamma}^* & \kappa_\beta \kappa_\gamma c_{1\beta 4\gamma}^* & 0 & 0 & 0 & 0 \\ \kappa_\beta \kappa_\gamma c_{2\beta 1\gamma}^* & \mathbf{F}_m(2, 2) & \kappa_\beta \kappa_\gamma c_{2\beta 3\gamma}^* & \kappa_\beta \kappa_\gamma c_{2\beta 4\gamma}^* & 0 & 0 & 0 & 0 \\ \kappa_\beta \kappa_\gamma c_{3\beta 1\gamma}^* & \kappa_\beta \kappa_\gamma c_{3\beta 2\gamma}^* & \mathbf{F}_m(3, 3) & \kappa_\beta \kappa_\gamma c_{3\beta 4\gamma}^* & 0 & 0 & 0 & 0 \\ \kappa_\beta \kappa_\gamma e_{\beta 1\gamma}^* & \kappa_\beta \kappa_\gamma e_{\beta 2\gamma}^* & \kappa_\beta \kappa_\gamma e_{\beta 3\gamma}^* & \kappa_\beta \kappa_\gamma e_{\beta 4\gamma}^* & 0 & 0 & 0 & 0 \\ -i\kappa_\beta c_{111\beta}^* & -i\kappa_\beta c_{112\beta}^* & -i\kappa_\beta c_{113\beta}^* & -i\kappa_\beta c_{114\beta}^* & 1 & 0 & 0 & 0 \\ -i\kappa_\beta c_{121\beta}^* & -i\kappa_\beta c_{122\beta}^* & -i\kappa_\beta c_{123\beta}^* & -i\kappa_\beta c_{124\beta}^* & 0 & 1 & 0 & 0 \\ -i\kappa_\beta c_{131\beta}^* & -i\kappa_\beta c_{132\beta}^* & -i\kappa_\beta c_{133\beta}^* & -i\kappa_\beta c_{134\beta}^* & 0 & 0 & 1 & 0 \\ -i\kappa_\beta e_{11\beta}^* & -i\kappa_\beta e_{12\beta}^* & -i\kappa_\beta e_{13\beta}^* & -i\kappa_\beta e_{14\beta}^* & 0 & 0 & 0 & 1 \end{bmatrix}, \tag{31}$$

$$\mathbf{F}_m(1, 1) = -\rho_0 \omega^2 + \kappa_\beta \kappa_\gamma \sigma_{\beta\gamma}^0 - i\kappa_\beta \sigma_{j\beta,j}^0 + \kappa_\beta \kappa_\gamma c_{1\beta 1\gamma}^*,$$

$$\mathbf{F}_m(2, 2) = -\rho_0 \omega^2 + \kappa_\beta \kappa_\gamma \sigma_{\beta\gamma}^0 - i\kappa_\beta \sigma_{j\beta,j}^0 + \kappa_\beta \kappa_\gamma c_{2\beta 2\gamma}^*,$$

$$\mathbf{F}_m(3, 3) = -\rho_0 \omega^2 + \kappa_\beta \kappa_\gamma \sigma_{\beta\gamma}^0 - i\kappa_\beta \sigma_{j\beta,j}^0 + \kappa_\beta \kappa_\gamma c_{3\beta 3\gamma}^*.$$

Eq. (29) can be solved easily and it has the solution

$$\mathbf{v}_m(x) = \mathbf{Q}_m \mathbf{R}_m(x) \mathbf{a}_m, \tag{32}$$

where

$$\mathbf{Q}_m = (h_{1m}, h_{2m}, h_{3m}, h_{4m}, h_{5m}, h_{6m}, h_{7m}, h_{8m}),$$

$$\mathbf{R}_m(x) = \text{diag}[\exp(b_{1m}x), \exp(b_{2m}x), \dots, \exp(b_{8m}x)],$$

$$\mathbf{a}_m = (a_{1m}, a_{2m}, \dots, a_{8m})^T. \tag{33}$$

h_{sm} and b_{sm} are the eigenvector components and eigenvalues of the state matrix, respectively. a_{sm} ($s = 1-8$) are undetermined constant coefficients in the sublayer m . The transfer matrix $\mathbf{P}_m(x_m - d_m, x_m)$ can be used to relate the displacements, stresses, electric displacements and electric potential at the bottom of the sublayer m to those at its top surface, i.e.,

$$\mathbf{v}_m(x_m - d_m) = \mathbf{P}_m(x_m - d_m, x_m)\mathbf{v}_m(x_m). \tag{34}$$

As a consequence of Eqs. (32)–(34), we are able to write the transfer matrix in the form

$$\mathbf{P}_m(x_m - d_m, x_m) = \mathbf{Q}_m \mathbf{R}_m(-d_m) \mathbf{Q}_m^{-1}, \tag{35}$$

where x_m is located in the bottom plane of the sublayer m . d_m is the thickness of the sublayer m .

Using the fundamental properties of the transfer matrix, we can find the relations as

$$\mathbf{P}(x', x) = \mathbf{P}(x', x'')\mathbf{P}(x'', x).$$

This leads to

$$\mathbf{P}(-h, 0) = \prod_{m=1}^N \mathbf{P}_m(x_m - d_m, x_m), \tag{36}$$

$$\mathbf{v}_N(-h) = \mathbf{P}(-h, 0)\mathbf{v}_1(0), \tag{37}$$

where $\mathbf{v}_N(-h)$ and $\mathbf{v}_1(0)$, respectively, are the state vectors at the upper and lower surfaces of the layer.

4. Propagation of Love waves in a prestressed transversely isotropic piezoelectric media

The structure, shown in Fig. 2, is two thin layers deposited on a substrate, where the thin layer SiO₂ is deposited on the substrate and ZnO is deposited on SiO₂ [11] (ZnO is the transversely isotropic piezoelectric medium, with five independent elastic constants, three piezoelectric coefficients, two dielectric constants and polarized along the z -axis and SiO₂ is isotropic elastic body with two independent elastic constants and one dielectric constant). Let the Love wave propagate in the positive direction of the y -axis. It is assumed that there only exist prestressed components $\sigma_y^0(x)$ ($\sigma_{22}^0(x)$) and $\sigma_z^0(x)$ ($\sigma_{33}^0(x)$), which are only the function of x , as shown in Fig. 2. The other stress components and Φ^0 are assumed to be zero. The components of mechanical displacement and the electric potential of Love wave satisfy

$$u = v = 0, \quad w = w(x, y, t), \quad \Phi = \Phi(x, y, t), \quad \kappa_y = \kappa, \quad \kappa_z = 0,$$

where u , v and w are the components of displacement along the x -, y - and z -axis, respectively.

Then for the Love wave, Eqs. (28), (30), (31) are simplified as

$$\mathbf{v}_m(x) = (A_{3m}, A_{4m}, T_{5m}, T_{7m})^T \tag{38}$$

and

$$\mathbf{B}_m(x) = \begin{bmatrix} i\kappa c_{45}^* & i\kappa e_{14}^* & 1 & 0 \\ i\kappa e_{25}^* & -i\kappa \epsilon_{21}^* & 0 & 1 \\ c_{55}^* & e_{15}^* & 0 & 0 \\ e_{15}^* & -\epsilon_{11}^* & 0 & 0 \end{bmatrix}, \tag{39}$$

where (according to Eqs. (17), (19) and $\Phi^0 = 0$)

$$\begin{aligned} c_{45}^* &= c_{3231} + c_{32n1}u_{3,n}^0 + c_{3n31}u_{2,n}^0, & e_{14}^* &= e_{132} + e_{13l}u_{2,l}^0 + e_{132kl}u_{k,l}^0, \\ e_{25}^* &= e_{231} + e_{23l}u_{1,l}^0 + e_{231kl}u_{k,l}^0, & \epsilon_{21}^* &= \epsilon_{21} + l_{21ij}u_{i,j}^0, \\ c_{55}^* &= c_{1313} + 2c_{13n3}u_{1,n}^0 + c_{1331mn}u_{m,n}^0, & e_{15}^* &= e_{113} + e_{131kl}u_{k,l}^0, \\ & & \epsilon_{11}^* &= \epsilon_{11} + l_{11ij}u_{i,j}^0 \end{aligned} \tag{40}$$

and

$$\mathbf{F}_m(x) = \begin{bmatrix} -\rho_0\omega^2 + [c_{44}^* + \sigma_y^0(x_m)]\kappa^2 & e_{24}^*\kappa^2 & 0 & 0 \\ e_{24}^*\kappa^2 & -\epsilon_{22}^*\kappa^2 & 0 & 0 \\ -i\kappa c_{54}^* & -i\kappa e_{25}^* & 1 & 0 \\ -i\kappa e_{14}^* & i\kappa \epsilon_{12}^* & 0 & 1 \end{bmatrix}, \tag{41}$$

where

$$\begin{aligned} c_{44}^* &= c_{3232} + c_{3232mn}u_{m,n}^0 + 2c_{23n2}u_{3,n}^0, & e_{24}^* &= e_{232} + e_{24l}u_{1,l}^0 + e_{241kl}u_{k,l}^0, \\ \epsilon_{22}^* &= \epsilon_{22} + l_{22ij}u_{i,j}^0, & c_{54}^* &= c_{1332} + c_{1332mn}u_{m,n}^0 + c_{1331}u_{3,2}^0, \\ e_{25}^* &= e_{213} + e_{23l}u_{1,l}^0 + e_{231kl}u_{k,l}^0, & \epsilon_{12}^* &= \epsilon_{12} + l_{12ij}u_{i,j}^0. \end{aligned} \tag{42}$$

Eqs. (38)–(42) are the general formulae for \mathbf{B}_m and \mathbf{F}_m in the propagation of Love wave in the prestressed piezoelectric media. But for ZnO and SiO₂, the coefficients c_{45} , e_{14} , e_{25} , ϵ_{21} , c_{54} , ϵ_{12} are zero and in the following discussions the initial displacement is assumed to be small. Neglecting the smaller terms, \mathbf{B}_m and \mathbf{F}_m can be, respectively, simplified as

$$\begin{aligned} \mathbf{B}_m(x) &= \begin{bmatrix} 0 & 0 & 1 & 0 \\ 0 & 0 & 0 & 1 \\ c_{55}^* & e_{15}^* & 0 & 0 \\ e_{15}^* & -\epsilon_{11}^* & 0 & 0 \end{bmatrix}, \\ \mathbf{F}_m(x) &= \begin{bmatrix} -\rho_0\omega^2 + [c_{44}^* + \sigma_y^0(x_m)]\kappa^2 & e_{24}^*\kappa^2 & 0 & 0 \\ e_{24}^*\kappa^2 & -\epsilon_{22}^*\kappa^2 & 0 & 0 \\ 0 & 0 & 1 & 0 \\ 0 & 0 & 0 & 1 \end{bmatrix}. \end{aligned} \tag{43}$$

About the ceramics from 6 mm class, we have $c_{55} = c_{44}$, $e_{24} = e_{15}$, $\epsilon_{11} = \epsilon_{22}$. So, the differences between c_{44}^* and c_{55}^* , e_{24}^* and e_{15}^* , ϵ_{22}^* and ϵ_{11}^* can be neglected. The eigenvalues of the state matrix $\mathbf{B}_m^{-1}(x)\mathbf{F}_m(x)$ may be obtained as

$$b_{1m,2m} = \pm\kappa, \quad b_{3m,4m} = \pm\kappa q_m, \quad q_m = \sqrt{1 - \frac{\rho c^2 - \sigma_y^0(x_m)}{\bar{c}_{55}}}, \tag{44}$$

where $\bar{c}_{55} = c_{55}^* + (e_{15}^*)^2/\epsilon_{11}^*$, c is the phase velocity and given by $c = \omega/\kappa$.

For the four eigenvalues, there are four four-component eigenvectors to compose the eigentensor \mathbf{Q}_m :

$$\mathbf{Q}_m = \begin{bmatrix} 0 & 0 & 1 & 1 \\ 1 & 1 & e_{15}^*/\epsilon_{11}^* & e_{15}^*/\epsilon_{11}^* \\ e_{15}^*\kappa & -e_{15}^*\kappa & \bar{c}_{55}q_m\kappa & -\bar{c}_{55}q_m\kappa \\ -\epsilon_{11}^*\kappa & \epsilon_{11}^*\kappa & 0 & 0 \end{bmatrix}. \tag{45}$$

Substituting Eqs. (41) and (43) into Eq. (32), the state vector at $x = x_m$ can be written as

$$\mathbf{v}_m(x_m) = \begin{bmatrix} 0 & 0 & 1 & 1 \\ 1 & 1 & e_{15}^*/\epsilon_{11}^* & e_{15}^*/\epsilon_{11}^* \\ e_{15}^*\kappa & -e_{15}^*\kappa & \bar{c}_{55}q_m\kappa & -\bar{c}_{55}q_m\kappa \\ -\epsilon_{11}^*\kappa & \epsilon_{11}^*\kappa & 0 & 0 \end{bmatrix} \times \begin{bmatrix} \exp(\kappa x_m) & & & \\ & \exp(-\kappa x_m) & & \\ & & \exp(\kappa q_m x_m) & \\ & & & \exp(-\kappa q_m x_m) \end{bmatrix} \begin{Bmatrix} a_{1m} \\ a_{2m} \\ a_{3m} \\ a_{4m} \end{Bmatrix}. \tag{46}$$

Then the transfer matrix of the sublayer m is (Eq. (35))

$$\mathbf{P}(x_m - d_m, x_m) = \begin{bmatrix} \cosh(\kappa q_m d_m) & 0 & -\frac{\sinh(\kappa q_m d_m)}{\bar{c}_{55}\kappa q_m} & -\frac{e_{15}^* \sinh(\kappa q_m d_m)}{\bar{c}_{55}\kappa q_m \epsilon_{11}^*} \\ P(2, 1) & \cosh(\kappa d_m) & -\frac{e_{15}^* \sinh(\kappa q_m d_m)}{\bar{c}_{55}\epsilon_{11}^* \kappa q_m} & P(2, 4) \\ P(3, 1) & -e_{15}^*\kappa \sinh(\kappa d_m) & \cosh(\kappa q_m d_m) & P(3, 4) \\ -\kappa e_{15}^* \sinh(\kappa d_m) & \epsilon_{11}^*\kappa \sinh(\kappa d_m) & 0 & \cosh(\kappa d_m) \end{bmatrix}, \tag{47}$$

$$P(2, 1) = \frac{e_{15}^*}{\epsilon_{11}^*} [\cosh(\kappa q_m d_m) - \cosh(\kappa d_m)], \quad P(2, 4) = \frac{\sinh(\kappa d_m)}{\epsilon_{11}^* \kappa} - \frac{e_{15}^* \sinh(\kappa q_m d_m)}{\bar{c}_{55}\kappa q_m \epsilon_{11}^{*2}},$$

$$\begin{aligned}
 P(3, 1) &= -\bar{c}_{55}\kappa q_m \sinh(\kappa q_m d_m) + \frac{e_{15}^{*2}\kappa \sinh(\kappa d_m)}{\epsilon_{11}^*}, \\
 P(3, 4) &= -\frac{e_{15}^*}{\epsilon_{11}^*} \cosh(\kappa d_m) + \frac{e_{15}^*}{\epsilon_{11}^*} \cosh(\kappa q_m d_m).
 \end{aligned}
 \tag{48}$$

It is well known that the Love wave motion is confined to the layers and region near the substrate surface. This requires that the component of displacement w and electric potential Φ remain finite when x tends to ∞ . Thus, the state vectors of the substrate can be founded as

$$\mathbf{v}_0(x) = \mathbf{Q}_0 \begin{Bmatrix} 0 \\ a_{2_0} \exp(b_{2_0}x) \\ 0 \\ a_{4_0} \exp(b_{4_0}x) \end{Bmatrix}.
 \tag{49}$$

The subscript label “0” is designated for the quantities in the substrate. The eigentensor of the substrate \mathbf{Q}_0 can be obtained by substitution of the material constants of the substrate into Eq. (45).

The vector at $x = 0$ becomes

$$\mathbf{v}_0(0) = \mathbf{Q}_0(0)(0, a_{2_0}, 0, a_{4_0})^T.
 \tag{50}$$

The electric potential Φ_{N+1} and electric displacement $D_x^{(N+1)}$ in the air ($x < -h$) can be expressed as

$$\Phi_{N+1}(x, t) = a_{N+1} \exp(\kappa x) \exp[i(\kappa_\alpha x_\alpha - \omega t)], \quad D_x^{(N+1)} = -\epsilon_0 \Phi_{N+1,x},
 \tag{51}$$

where a_{N+1} is the undetermined coefficient and ϵ_0 is the dielectric constant of air.

The waves must satisfy the appropriate electrical and mechanical boundary conditions at the surface of the layer and continuity conditions between the interface of the layer and the substrate.

The mechanical boundary conditions are

$$\sigma_{zx} = 0 \quad \text{at } x = -h,
 \tag{52a}$$

$$[\sigma_{zx}] = 0, \quad [w] = 0 \quad \text{at } x = 0,
 \tag{52b}$$

where $[\sigma_{zx}] = \sigma_{zx+} - \sigma_{zx-}$, $[w] = w_+ - w_-$ on the interface.

The metalization on the surface of the layer is assumed to consist of a perfectly conducting film of negligible thickness and this corresponds to an electrically shorted condition. The presence of the metal film has no influence on the mechanical boundary conditions [21]. The other case is the surface electrically free. In these two cases the electrical boundary conditions are

$$D_x = D_x^{(N+1)}, \quad \Phi = \Phi_{N+1} \quad \text{at } x = -h \text{ (electrically free),}
 \tag{53a}$$

$$\Phi = 0 \quad \text{at } x = -h \text{ (electrically shorted),}
 \tag{53b}$$

$$[D_x] = 0, \quad [\Phi] = 0 \quad \text{at } x = 0.
 \tag{53c}$$

The continuity conditions at $x = 0$ can be expressed by the state vector

$$\mathbf{v}_1(0) = \mathbf{v}_0(0). \tag{54}$$

From Eqs. (36), (37), (50), (54), one can obtain the state vectors at the top surface of the layer:

$$\mathbf{v}_N(-h) = \mathbf{P}(-h, 0)\mathbf{v}_0(0) = \prod_{m=1}^N \mathbf{P}_m(x_m - dx_m, x_m)\mathbf{Q}_0(0, a_{20}, 0, a_{40})^T. \tag{55a}$$

Let

$$\mathbf{E} = \prod_{m=1}^N \mathbf{P}(x_m - dx_m, x_m)\mathbf{Q}_0. \tag{55b}$$

For electrically free surface one can get

$$\begin{Bmatrix} A_{3N} \\ A_{4N} \\ T_{5N} \\ T_{7N} \end{Bmatrix} = \begin{bmatrix} E_{11} & E_{12} & E_{13} & E_{14} \\ E_{21} & E_{22} & E_{23} & E_{24} \\ E_{31} & E_{32} & E_{33} & E_{34} \\ E_{41} & E_{42} & E_{43} & E_{44} \end{bmatrix} \begin{Bmatrix} 0 \\ a_{20} \\ 0 \\ a_{40} \end{Bmatrix} = \begin{Bmatrix} w_{N+1} \\ a_{N+1} \exp(-\kappa h) \\ 0 \\ -\epsilon_0 a_{N+1} \kappa \exp(-\kappa h) \end{Bmatrix}. \tag{55c}$$

It can be simplified as

$$\begin{Bmatrix} A_{4N} \\ T_{5N} \\ T_{7N} \end{Bmatrix} = \begin{bmatrix} E_{22} & E_{24} \\ E_{32} & E_{34} \\ E_{42} & E_{44} \end{bmatrix} \begin{Bmatrix} a_{20} \\ a_{40} \end{Bmatrix} = \begin{bmatrix} \exp(-\kappa h) \\ 0 \\ -\epsilon_0 \kappa \exp(-\kappa h) \end{bmatrix} \{a_{N+1}\}. \tag{56}$$

Eq. (56) can be rewritten as

$$\begin{bmatrix} E_{22} & E_{24} & -\exp(-\kappa h) \\ E_{32} & E_{34} & 0 \\ E_{42} & E_{44} & \epsilon_0 \kappa \exp(-\kappa h) \end{bmatrix} \begin{Bmatrix} a_{20} \\ a_{40} \\ a_{N+1} \end{Bmatrix} = 0. \tag{57}$$

To obtain nontrivial solutions for a_{20} , a_{40} and a_{N+1} the determinant of their coefficients should be vanished. The velocity is thus found by searching for the value of c that makes the determinant of the coefficient matrix equal to zero. So phase velocity equation for the electrically free case is

$$(E_{42} + \kappa \epsilon_0 E_{22})E_{34} - (E_{44} + \kappa \epsilon_0 E_{24})E_{32} = 0. \tag{58}$$

In a way similar to the electrically shorted case, we obtain a set of two homogeneous equations for the electrically shorted case:

$$\begin{Bmatrix} A_{4N} \\ T_{5N} \end{Bmatrix} = \begin{bmatrix} E_{22} & E_{24} \\ E_{32} & E_{34} \end{bmatrix} \begin{Bmatrix} a_{20} \\ a_{40} \end{Bmatrix} = \begin{Bmatrix} 0 \\ 0 \end{Bmatrix}. \tag{59}$$

The phase velocity is obtained when the coefficient determinant of a_{20} and a_{40} vanishes, or

$$E_{22}E_{34} - E_{32}E_{24} = 0. \tag{60}$$

5. The distributions of the initial stresses

The initial stresses in layers exist due to the manufacturing process or other reasons. The initial stresses $\sigma_{yZnO}^0, \sigma_{zZnO}^0, \sigma_{ySiO_2}^0, \sigma_{zSiO_2}^0$ must satisfy certain relations on the interface. At the interface between the SiO₂ layer and the ZnO, the initial displacements u^0, v^0 and their derivatives in the interface must be continuous, so the strains satisfy

$$\begin{aligned} \varepsilon_{yZnO}^0 &= \varepsilon_{ySiO_2}^0 = \varepsilon_y^0, \\ \varepsilon_{zZnO}^0 &= \varepsilon_{zSiO_2}^0 = \varepsilon_z^0, \\ \varepsilon_{yzZnO}^0 &= \varepsilon_{yzSiO_2}^0 = \varepsilon_{yz}^0. \end{aligned} \tag{61}$$

Because the material ZnO is transversely isotropic and SiO₂ is isotropic, then at $x = -h_1$ we have

$$\begin{aligned} \sigma_{xZnO}^0 &= c_{11}\varepsilon_{xZnO}^0 + c_{12}\varepsilon_y^0 + c_{13}\varepsilon_z^0 = 0, \\ \sigma_{yZnO}^0 &= c_{12}\varepsilon_{xZnO}^0 + c_{11}\varepsilon_y^0 + c_{13}\varepsilon_z^0, \quad \sigma_{zZnO}^0 = c_{13}\varepsilon_{xZnO}^0 + c_{13}\varepsilon_y^0 + c_{33}\varepsilon_z^0, \\ E\varepsilon_y^0 &= \sigma_{ySiO_2}^0 - \nu\sigma_{zSiO_2}^0, \quad E\varepsilon_z^0 = \sigma_{zSiO_2}^0 - \nu\sigma_{ySiO_2}^0, \end{aligned} \tag{62}$$

where $c_{11}, c_{12}, c_{13}, c_{33}$ are elastic coefficients of ZnO and E, ν are the modulus of elasticity and Poisson’s ration of SiO₂, respectively. According to Eq. (62), at $x = -h_1$ one obtains the following relations:

$$\sigma_{yZnO}^0(-h_1) = \frac{c_{11}^2 - c_{12}^2 - \nu c_{13}(c_{11} - c_{12})}{Ec_{11}} \sigma_{ySiO_2}^0(-h_1) + \frac{c_{13}(c_{11} - c_{12}) - \nu(c_{11}^2 - c_{12}^2)}{Ec_{11}} \sigma_{zSiO_2}^0(-h_1). \tag{63}$$

In the following, for convenience, it is assumed that $\sigma_{zSiO_2}^0(-h_1) = L\sigma_{ySiO_2}^0(-h_1) = L\sigma_y^{(1)}$, where L is a proportional coefficient of $\sigma_{zSiO_2}^0(-h_1)$ to $\sigma_{ySiO_2}^0(-h_1)$. Then we can get

$$\begin{aligned} \sigma_{yZnO}^0(-h_1) &= a\sigma_y^{(1)}, \\ a &= \frac{(1 - L\nu)(c_{11}^2 - c_{12}^2) + c_{13}(L - \nu)(c_{11} - c_{12})}{Ec_{11}}. \end{aligned} \tag{64}$$

σ_{zZnO}^0 can also be obtained from the third of Eq. (62), but it is not discussed here because it does not enter Eq. (43) in the present special case. We assume that the initial stresses $\sigma_{yZnO}^0, \sigma_{ySiO_2}^0$ and $\sigma_{zSiO_2}^0$ are only the exponential functions of x and they are similar functions, which reach the maximum at the top surface of layer ZnO and are zero at the substrate, as shown in Fig. 2.

When $h_1 \neq 0$

$$\begin{aligned} \sigma_{ySiO_2}^0(x) &= f(x) = \frac{\sigma_y^{(1)}}{e^{-h_1} - 1} (e^x - 1), \quad -h_1 \leq x \leq 0, \\ \sigma_{yZnO}^0(x) &= g(x) = \frac{\sigma_y^{(2)}}{e^{-h} - 1} (e^x - 1), \quad -h \leq x \leq -h_1, \end{aligned} \tag{65}$$

where $\sigma_y^{(2)} = \sigma_{yZnO}^0(-h)$.

According to Eqs. (64), (65) one obtains

$$\sigma_{y_{\text{SiO}_2}}^0(x) = f(x) = \frac{\sigma_y^{(2)}}{a(e^{-h} - 1)} (e^x - 1). \tag{66}$$

When $h_1 = 0$

$$\sigma_{y_{\text{ZnO}}}^0(x) = g(x) = \frac{\sigma_y^{(2)}}{e^{-h} - 1} (e^x - 1). \tag{67}$$

When there are no initial stresses, the phase velocity c of Love waves is

$$(c_{\text{shZnO}}, c_{\text{shSiO}_2})_{\min} < c < c_{\text{shSi}},$$

where

$$c_{\text{shZnO}} = \sqrt{(c_{55} + e_{15}^2/\epsilon_{11})/\rho_{\text{ZnO}}},$$

$c_{\text{shSiO}_2} = \sqrt{\mu_{\text{SiO}_2}/\rho_{\text{SiO}_2}}$ and $c_{\text{shSi}} = \sqrt{\mu_{\text{Si}}/\rho_{\text{Si}}}$, respectively, are the shear bulk velocities of the ZnO, SiO₂ layer and the substrate.

6. Numerical examples

In the following numerical examples h_2 is fixed and equal to 1×10^{-5} m. By changing the value of h_1 in a wide range and $\sigma_y^{(2)}$, we can obtain a series of phase and group velocities. From the results it is seen that the phase and group velocities can be adjusted in a larger range when the SiO₂ layer exists. The material constants are shown in Tables 1 and 2 and $c_{\text{shSi}} = \sqrt{\mu_{\text{Si}}/\rho_{\text{Si}}} = 5840$ m/s, $c_{\text{shSiO}_2} = \sqrt{\mu_{\text{SiO}_2}/\rho_{\text{SiO}_2}} = 3765.9$ m/s, $c_{\text{shZnO}} = \sqrt{(c_{55} + e_{15}^2/\epsilon_{11})/\rho_{\text{ZnO}}} = 2841.5$ m/s.

Figs. 3a and b show the relations between the phase velocity c_0 , group velocity c_{g_0} of the Love wave and κh , respectively, for the electrically free case without initial stress, where $c_{g_0} = \frac{d\omega}{d\kappa} =$

Table 1
Material constants of ZnO

Density (10^3 kg/m ³)	Elastic constants (10^{10} N/m ²)				Piezoelectric constants (C/m ²)			Dielectric constants (10^{-10} F/m)	
	c_{11}	c_{12}	c_{13}	c_{44}	e_{15}	e_{31}	e_{33}	ϵ_{11}	ϵ_{33}
5.665	20.96	12.05	10.46	4.23	-0.48	-0.573	1.321	0.67	0.799

Table 2
The Lamé' constants of Si and SiO₂

Material	Lamé' constants (10^{10} N/m ²)		Density (10^3 kg/m ³)	Dielectric constants (10^{-10} F/m)	
	λ	μ		ϵ_{11}	ϵ_{33}
Si	16.57	7.94	2.328	1.035	1.035
SiO ₂	7.85	3.12	2.2	0.33	0.33

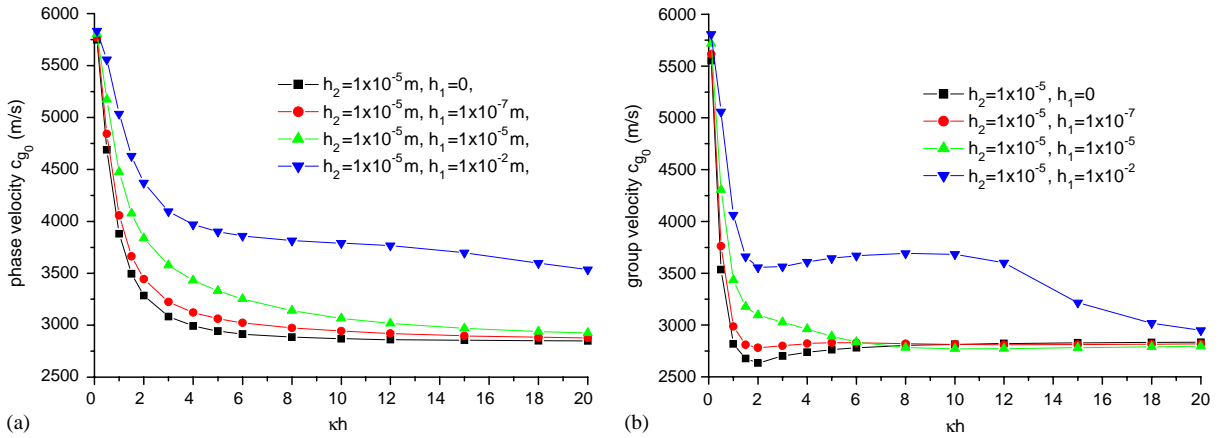


Fig. 3. (a) Phase velocity with κh for the electrically free case without initial stresses and $L = 1$, (b) group velocity with κh for the electrically free case without initial stresses and $L = 1$.

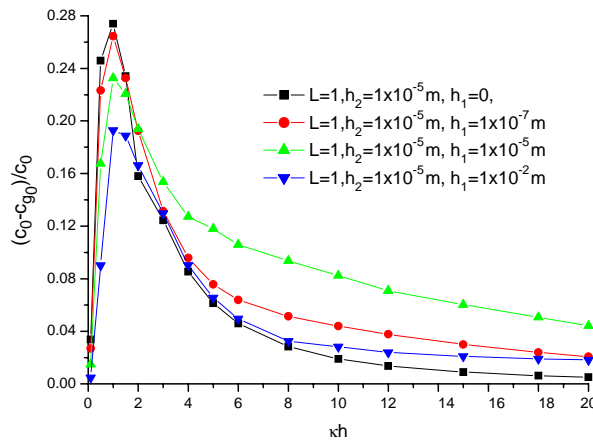


Fig. 4. Variations of velocity change $(c_0 - c_{g0})/c_0$ with κh for the electrically free case without initial stresses.

$\frac{d(c_0 \kappa)}{d\kappa} = c_0 + \kappa \frac{dc_0}{d\kappa}$ (the c_{g0} curves are not smooth due to the differentiation, $dc_0/d\kappa$, in it). In these cases the phase and group velocities will decrease with the increasing κh for a given value of h_1 and the curves tend asymptotically to a horizontal line as $\kappa h \rightarrow \infty$. These results show that the velocities of the Love wave are a function of κh , i.e. Love wave is a dispersion wave in a layered structure. For all h_1 values we have $c \rightarrow c_{shSi}$ for $\kappa h \rightarrow 0$. For $\kappa h \rightarrow \infty$ we have $c \rightarrow c_{shZnO}$ when h_1 is the same or less than the order of h_2 . But c will approach c_{shSiO_2} when h_1 is much larger than h_2 and this means that in this case the layer has the property as SiO_2 . The thickness h_1 of the middle layer SiO_2 affects the phase and group velocities significantly and they increase with increasing h_1 . So, by adjusting h_1 we can change the velocities in a wide range than that in the case without the middle layer.

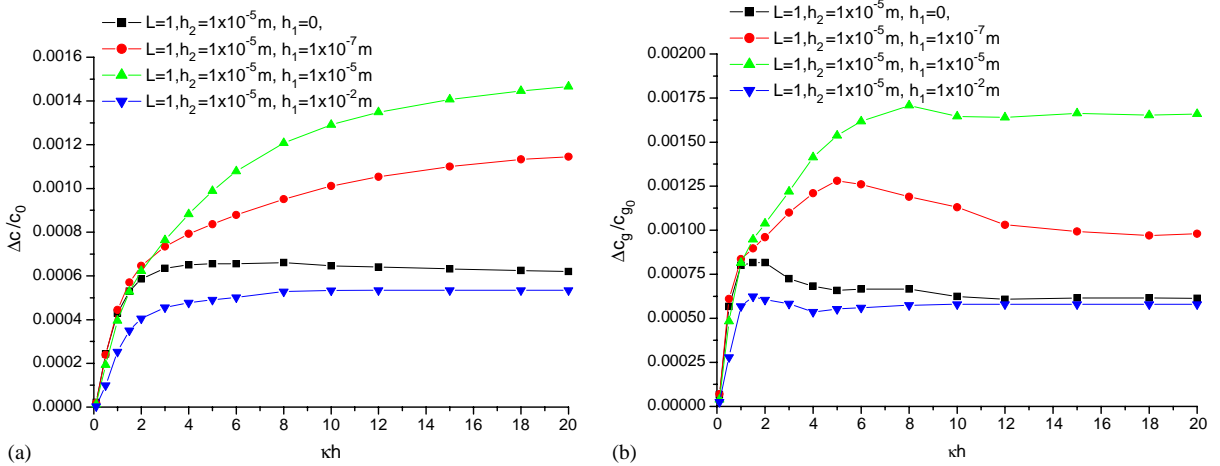


Fig. 5. (a) Variations of phase velocity change $\Delta c/c_0$ with κh and $\sigma_y^{(2)} = +200$ MPa for the electrically free case, (b) variations of phase velocity change $\Delta c_g/c_{g_0}$ with κh and $\sigma_y^{(2)} = +200$ MPa for the electrically free case.

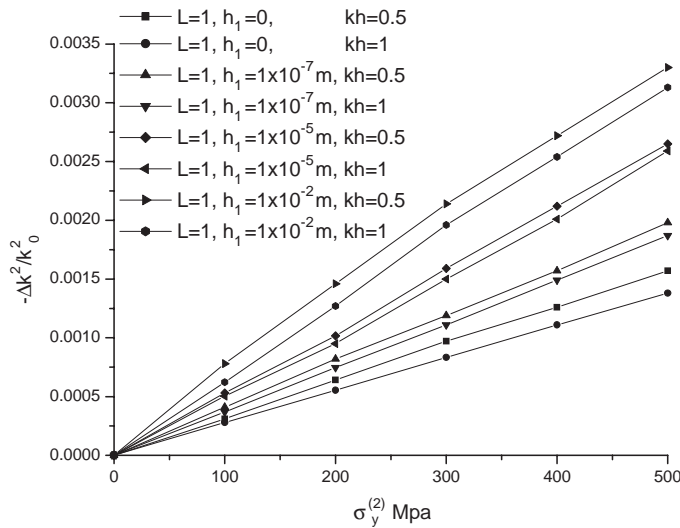


Fig. 6. Variation of the electromechanical coupling coefficient κ^2 with $\sigma_y^{(2)}$ and $h_2 = 1 \times 10^{-5}$ m.

Fig. 4 shows variations of $(c_0 - c_{g_0})/c_0$ with κh for the electrically free case without initial stresses. In the discussed cases the difference between c_0 and c_{g_0} achieves its maximum value in the range $0.5 < \kappa h < 2$. When $h_1/h_2 \rightarrow 0$ or ∞ the difference between c_0 and c_{g_0} has a smaller value compared with finite h_1/h_2 . So, the energy propagation velocity is obviously slower than the phase velocity when h_1 has the same order as h_2 .

Figs. 5a and b show the relations of relative variation of the phase velocity $\Delta c/c_0$ and group velocity $\Delta c_g/c_{g_0}$ with κh for the case with initial stresses. When the initial stress is positive stress, in

general, the value of $\Delta c/c_0$ and $\Delta c_g/c_{g_0}$ increase with increasing κh and the curves tend asymptotically to a horizontal line as $\kappa h \rightarrow \infty$, where $\Delta c = c - c_0$, $\Delta c_g = c_g - c_{g_0}$. c , c_0 and c_g , c_{g_0} are phase and group velocities with and without initial stress, respectively. It is seen that $h_1/h_2 \rightarrow 0$ or ∞ , $\Delta c/c_0$ or $\Delta c_g/c_{g_0}$ is smaller than that of finite h_1/h_2 . The maximum value is arrived when h_1/h_2 have the same order.

Fig. 6 shows the variation of the electromechanical coupling coefficient κ^2 with $\sigma_y^{(2)}$ and h_1 . $\kappa^2 = 2(c_f - c_s)/c_f$, where c_f and c_s are the phase velocities of electrically free and shorted cases, respectively. $\Delta\kappa^2 = \kappa^2 - \kappa_0^2$, where κ_0^2 is the value of κ^2 in the case without initial stress. When the initial stress and the thickness of the middle layer (SiO_2) increase the value $-(\Delta\kappa^2/\kappa_0^2)$ increases, too. It is also found that the relation c_s with κh is similar to c_f , but c_f is larger than c_s at the same κh .

7. Conclusions

Generally, we use the fractional change in phase $\Delta\phi/\phi$, frequency $\Delta f/f$ or velocity $\Delta c/c$ to reflect the acoustoelastic effect of surface acoustic waves. They are given by the relations $\Delta c/c = s_p - \Delta\phi/\phi$ and $\Delta c/c = \Delta f/f$, where s_p is the strain in the direction of propagation. $\Delta\phi/\phi$ can be measured by the phase shift detection technique. So, it is valuable to compute the phase velocities.

In this paper, the fundamental governing equations and boundary conditions Eqs. (20) and (21), for a general prestressed piezoelectric media under finite deformation, are established. The global state vector equations (38)–(42) for Love wave in the layer prestressed piezoelectric materials are also established. Under the small prestressed conditions the variations of phase velocity, group velocity and coupling coefficient with the thickness of middle layer and initial stress are discussed in detail. The theoretical and numerical results of this paper are meaningful and helpful to improve the behavior of the SAW devices.

Acknowledgements

This work is supported by the National Science Foundation through Grants No. 10472069 and No. 10132010.

References

- [1] A.H. Nayfeh, The general problem of elastic wave propagation in multilayered anisotropic media, *Journal of Acoustical Society of America* 89 (1991) 1521–1531.
- [2] W.T. Thomson, Transmission of elastic waves through a stratified solid medium, *Journal of Applied Physics* 21 (1950) 89–93.
- [3] G.R. Liu, J. Tani, K. Watanabe, T. Ohyoshi, Lamb wave propagation in anisotropic laminates, *ASME Journal of Applied Mechanics* 57 (1990) 923–929.
- [4] G.R. Liu, J. Tani, Surface waves in functionally gradient piezoelectric material plates, *ASME Journal of Vibration and Acoustics* 116 (1994) 440–448.
- [5] J.T. Stewart, Y.K. Yong, Exact analysis of the propagation of acoustic waves in multilayered anisotropic piezoelectric plates, *IEEE Transactions on Ultrasonics Ferroelectrics and Frequency Control* 41 (1994) 375–390.

- [6] D. Levesque, L. Piche, A robust transfer matrix formulation for the ultrasonic response of multilayered absorbing media, *Journal of Acoustical Society of America* 92 (1992) 452–467.
- [7] M.J.S. Lowe, Matrix techniques for modeling ultrasonic waves in multilayered media, *IEEE Transactions on Ultrasonics Ferroelectrics and Frequency Control* 42 (1995) 525–542.
- [8] H. Liu, Z.B. Kuang, Z.M. Cai, Application of transfer method in analyzing the inhomogenous initial stress problem in prestressed layered piezoelectric media, in: K. Watanabe, F. Zigler (Eds.), *IUTAM Symposium on Dynamics of Advanced Materials and Smart Structures*, 2003.
- [9] A.L. Nalamwar, M. Epstein, Surface acoustic waves in strained media, *Journal of Applied Physics* 47 (1976) 43–48.
- [10] S. Ono, K. Wasa, S. Hayakawa, Surface-acoustic-wave properties in ZnO–SiO₂–Si layered structure, *Wave Electronics* 3 (1977) 35–49.
- [11] A.K. Sinha, W.J. Tanski, T. Lukaszek, A. Ballato, Influence of biasing stress on the propagation of surface waves, *Journal of Applied Physics* 57 (1985) 767–776.
- [12] H.F. Tiersten, Perturbation theory for linear electroelastic equations for small fields superposed on a bias, *Journal of Acoustical Society of America* 64 (1978) 832–837.
- [13] J. Du, G.L. Harding, J.A. Ogilvy, P.R. Dencher, M. Lake, A study of Love wave acoustic sensors, *Sensors and Actuators A* 56 (1996) 211–219.
- [14] M.X. Deng, The effects of the *c*-axis orientation of the ZnO film and other parameters in ZnO–SiO₂–Si layered structure on SAW, *Applied Acoustics* 16 (1996) 18–23 (in Chinese).
- [15] B.T. Khuri-Yakub, G.S. Kino, A monolithic Zinc–Oxide–Silicon convolver, *Applied Physics Letters* 25 (1974) 188–193.
- [16] M.B. Assour, O. Elmazria, R.J. Riobóo, F. Sarry, P. Alnot, Modelling of SAW filter based on ZnO/diamond/Si layered structure including velocity dispersion, *Applied Surface Science* 164 (2000) 200–204.
- [17] Z.B. Kuang, *Nonlinear Continuum Mechanics*, Shanghai Jiaotong University Press, Shanghai, 2002.
- [18] Y.H. Pao, W. Sachse, H. Fukuoka, Acoustoelasticity and ultrasonic measurements of residual stresses, in: W.P. Mason, R.N. Thurston (Eds.), *Physical Acoustics*, vol. XVII, New York, 1984, p. 62.
- [19] H. Liu, Z.B. Kuang, Z.M. Cai, Propagation of Bleustein–Gulyaev waves in a prestressed layered piezoelectric structure, *Ultrasonics* 41 (2003) 397–405.
- [20] H. Fahmy, E.L. Adler, Propagation of acoustic surface waves in multilayers: a matrix description, *Applied Physics Letters* 22 (1973) 495–497.
- [21] S.G. Joshi, Y. Jin, Propagation of ultrasonic Lamb waves in piezoelectric plates, *Journal of Applied Physics* 70 (1991) 4113–4120.